

H103

PRESSURE DROP AND HEAT TRANSFER OF ARRAYS OF IN-LINE
CIRCULAR BLOCKS ON THE WALL OF PARALLEL CHANNEL

Tamotsu IGARASHI*, Hajime NAKAMURA* and Taketo FUKUOKA*

* Department of Mechanical Engineering, The National Defense Academy
1-10-20 Hashirimizu, Yokosuka, 239-0811 Japan

ABSTRACT Pressure drop and heat transfer of arrays of in-line circular blocks on the wall of parallel channel were measured. The diameter and height of the block were 40 mm and 18 mm, respectively. The pitches of the block were varied. The effects of the number of line and row and the other factors on the pressure loss and heat transfer were clarified. The coefficient of loss ζ can be formulated and the recommended equation agrees with the experimental data within $\pm 10\%$. The average heat transfer coefficient of the block of 1st row is lower than that of 2nd row. Those of 1st to 5th rows are nearly equal and can be approximately expressed by the following equation: $Num = 0.118 (Re/\beta)^{0.75}$, where β is the opening ratio.

Key words: Pressure Loss, Heat Transfer, Circular Blocks, In-line Arrangement

1. INTRODUCTION

According to the air cooling design of electronic equipment [1], the pressure drop and heat transfer performance of the equipment are important factors. In the previous papers [2, 3], the matter are not reached. The authors [4] carried out experimental studies on the pressure loss of arrays of in-line square blocks having practical size on the wall of parallel channel. The height of block, number of lines and rows, and pitches of the block were systematically varied. The pressure drop coefficient is given by the sum of the pressure drop of three regions: the inlet, intermediate and outlet ports.

In the present study, the pressure loss and the average heat transfer of arrays of in-line circular blocks on the wall of parallel channel were measured for various arrangements. The pressure loss coefficient is formulated by the same method as the previous paper [4]. And the average Nusselt numbers of the blocks are given by the general equations. Those recommended equations agree with the experimental data within $\pm 10\%$. Finally, the average Nusselt number is correlated to the pressure loss coefficient and is given by the dimensionless expression. This fact enables the prediction of the pressure loss of the arrays of circular blocks.

2. EXPERIMENTAL APPARATUS AND PROCEDURE

The schematic of test section and symbols are shown in Fig. 1. The test section having height $B = 30$ mm, wide $W = 250$ mm and length $L = 250$ mm was made of acrylic resin. The circular blocks having diameter $d = 40$ mm and height $H = 18$ mm are made of aluminium and positioned along the lower wall in an in-line arrangement. The pitches of the blocks, P_1 and P_2 , were varied from 50 to 80 mm, respectively. The number of lines M was varied from 5 to

3 and that of rows N varied from 5 to 2. The flow around the blocks was visualized by an oil-flow method at $Um = 10$ m/s. The pressure distribution on the upper wall having many pressure taps of 0.6 mm in diameter was measured using by an inclined manometer at $Um = 10$ m/s. From the results of Matsushima, et al. [3], the pressure drop is proportional to Um^2 , therefore, the pressure loss coefficient is independent of Reynolds number [4]. In the heat transfer measurement, the surface temperature around the blocks containing a heater was measured with 6 C-C thermocouples. The temperature difference between the maximum and the minimum values was less than 1°C . The mean value of surface temperature was defined to be θ_w . The average heat transfer coefficient of the block was obtained by $hm = q/(\theta_w - \theta_0)$. To clarify the Reynolds number effect on the Nusselt number, the mean velocity Um was set over a range from 2 to 10 m/s.

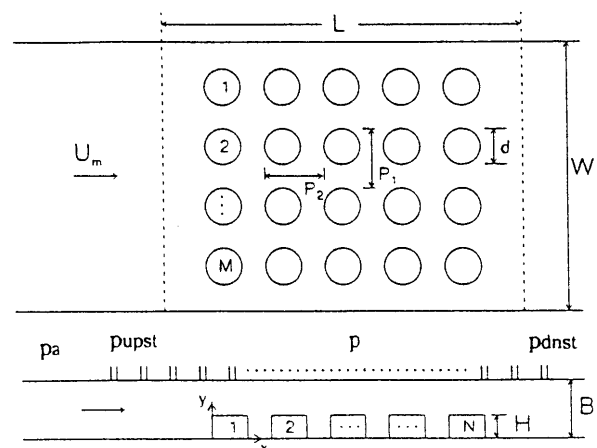


Fig. 1 Test section and symbols

3. PRESSURE DROP

3.1 Flow around array of blocks

Figure 2 shows examples of the surface oil-flow patterns on the blocks and the base plate. In the case of $M = N = 3$, the horseshoe vortices are formed on the base plate around the blocks. And the white crescent-shaped pattern appears on the 1st row block, which indicates the existence of the leading edge separation bubble. The large horseshoe vortices are formed on the base plate around the 2nd row block, but the crescent-shaped pattern disappear on the 2nd row block. The oil-flow patterns around the 3rd row block are similar to those of the upstream blocks. On the contrary, the flow on the side face of the blocks separate and the separation point goes downstream as the upper part. In the case of $M = N = 4$, the imperfect horseshoe vortices are formed ahead of individual block from 1st to last row. For the case of $M = N = 5$, the imperfect horseshoe vortices are also formed ahead of individual block, and that of second row is larger than those of other rows. This fact indicates that the heat transfer coefficient of the 2nd row is higher than that of first row. Moreover, the down-wash [5] can not be observed, which appeared from the top face to downstream region on the side face of a circular block in a boundary layer.

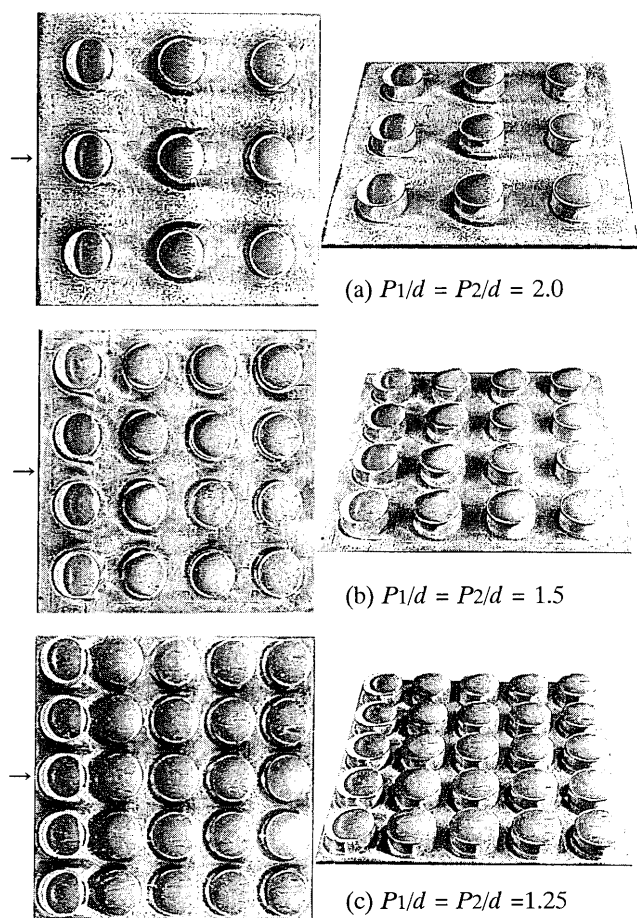


Fig. 2 Surface oil-flow patterns:
 $d = 40$ mm, $H = 18$ mm, $U_m = 10$ m/s

3.2 Pressure distribution and pressure loss coefficient

The effect of pitch P_1 on the pressure distribution on the upper wall is shown in Fig. 3. The pressure coefficient at the inlet of the 1st row block decreases suddenly by a vena contracta, and the pressure drop is remarkably large with a decrease in P_1 . The pressure coefficient decreases gradually on the downstream blocks, then the coefficient recovers at the outlet of the blocks. We try the formulation of the pressure loss coefficient ζ in the same manner as the previous report [4]. As shown in Fig. 4, the pressure loss coefficient is divided into three pressure coefficients at the inlet part of the 1st block, C_{p1} , between first and last blocks, C_{p2} , and at the downstream the last block, C_{p3} .

$$\zeta = (p_{upst} - p_{dnst}) / 0.5\rho U_m^2 \quad (1)$$

$$= [(p_{upst} - p_1) + (p_1 - p_2) + (p_2 - p_{dnst})] / 0.5\rho U_m^2$$

$$\zeta = C_{p1} + C_{p2} - C_{p3} \quad (2)$$

The above three coefficients are represented using the following dimensionless dominant factors.

$$C_{p1}, C_{p2}, C_{p3} = f(H/d, H/B, W/d, P_1/d, P_2/d, M, N) \quad (3-1)$$

We introduce the opening ratio, $\beta = 1 - (Hd/BW)M$ and the dominant factor $\delta = (1 - \beta) / \beta^2$, which was obtained in the hydraulic losses of flow control devices [5, 6]. We rewrite Eq. (3-1) as follows:

$$C_{p1}, C_{p2}, C_{p3} = f(\delta, P_1/d, P_2/d, N) \quad (3-2)$$

3.3 Formulation of pressure drop coefficient

3.3.1 Pressure drop at inlet part

The effects of N , δ and P_2/d on the C_{p1} are shown in Fig. 5. The effect of N can be neglected, and that of δ is expressed by $C_{p1} \propto \delta^{0.76}$. The value of C_{p1} decreases

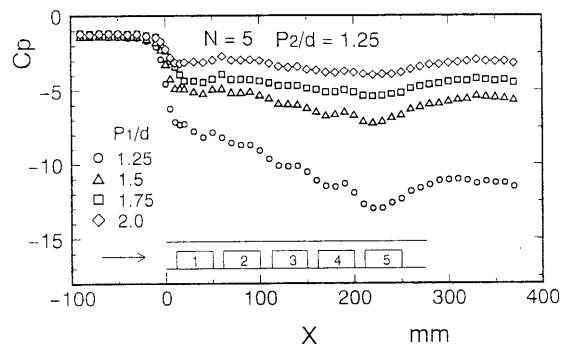


Fig. 3 Pressure distributions

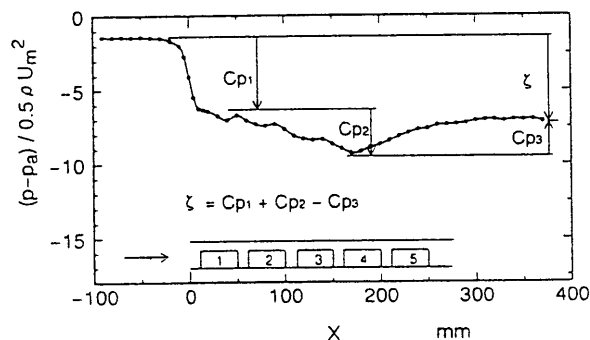


Fig. 4 Division of pressure drop

slightly with an increase in P_2/d and is expressed by $Cp_1 \propto (P_2/d)^{-0.23}$. We lead the following equation:

$$Cp_1 = 2.86 \delta^{0.76} (P_2/d)^{-0.23} \quad (4)$$

3.3.2 Pressure raise at outlet part

Figure 6 shows the effects of N , δ and P_2/d on the pressure raise coefficient at the outlet part Cp_3 . The effect of N on Cp_3 is given by $Cp_3 \propto (N - 1)^{0.09}$. Then, the effects of δ and P_2 are represented as $Cp_3 \propto \delta^{0.47}$ and $Cp_3 \propto (P_2/d)^{-0.18}$, respectively. Next, the constant value defined by $Cp_3/\delta^{0.47} [(N-1)/(P_2/d)^2]^{0.09}$ is averaged for all data. Finally, we lead the following equation:

$$Cp_3 = 1.13 \delta^{0.47} [(N - 1)/(P_2/d)^2]^{0.09} \quad (5)$$

3.3.3 Pressure drop between inlet and outlet parts

Figure 7 shows the effects of N , δ and P_2/d on the pressure drop coefficient between inlet and outlet parts, Cp_2 . We express the effects of N and P_2/d by the function $[(N - 1)/(P_2/d - 1)]$, the correlation obtained is $Cp_2 \propto [(N - 1)/(P_2/d - 1)]^{0.47}$. The effect of δ is given by $Cp_2 \propto \delta^{0.86}$. We neglect the effect of P_1/d on Cp_2 . The constant value defined by $Cp_2/\delta^{0.86} [(N - 1)/(P_2/d - 1)]^{0.47}$ is also averaged for all data. We lead the following equation:

$$Cp_2 = 1.40 \delta^{0.86} [(N - 1)/(P_2/d - 1)]^{0.47} \quad (6)$$

3.4 Recommended equation for pressure drop coefficients

The pressure drop coefficients and pressure raise coefficient for three parts are given by Eqs. (4) to (6), respectively. The individual recommended values obtained by the above equations agree well with the experimental values within $\pm 10\%$. Thus, the recommended value of the pressure loss coefficient of the array of blocks can be obtained by substituting Eqs. (4) to (6) into Eq. (2). As shown in Fig. 8, the recommended values agrees well with the experimental values within $\pm 10\%$.

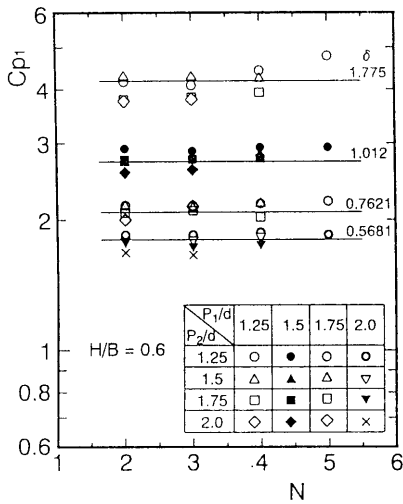
4. HEAT TRANSFER CHARACTERISTICS

4.1 Average heat transfer of arrays of circular blocks

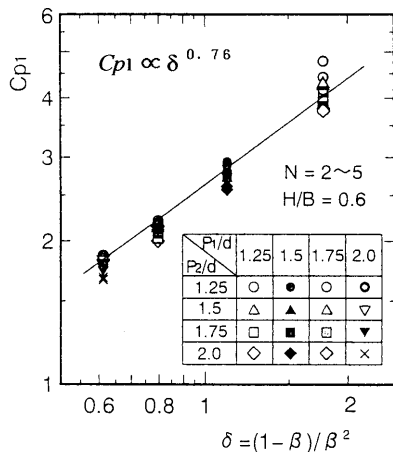
The average heat transfer of single circular block and that of array of in-line blocks for the cases $M = N = 3$ and $M = 3, N = 5$ are shown in Fig. 9 (a) and (b), respectively. The average Nusselt number of single block is given by

$$Num = 0.13 Re^{0.75} \quad (\text{single block}) \quad (7)$$

where, $Num = hmd/\lambda$, $Re = Umd/\nu$. The two broken lines in Fig. 9 (a) are correspond to those of single circular block having $d = 80$ mm and $H = 28$ mm in a laminar and turbulent boundary layers [5], respectively.

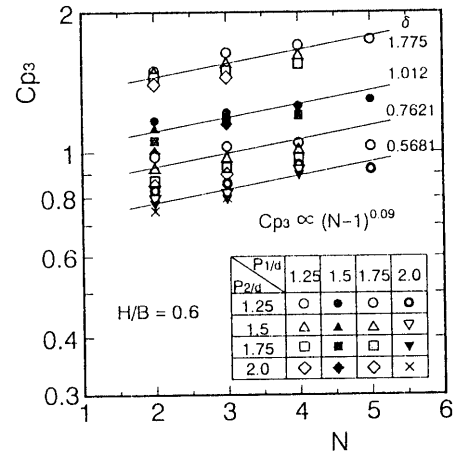


(a) Correlation of Cp_1 vs N

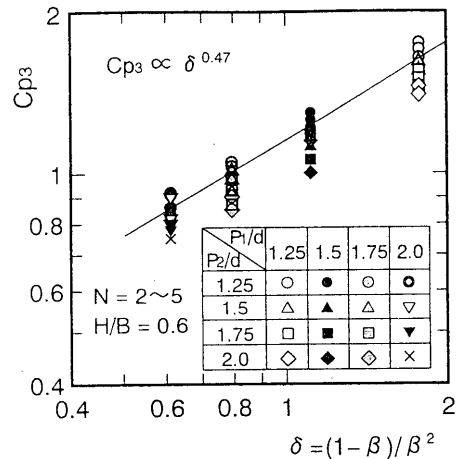


(b) Correlation of Cp_1 vs δ

Fig. 5 Pressure drop at inlet

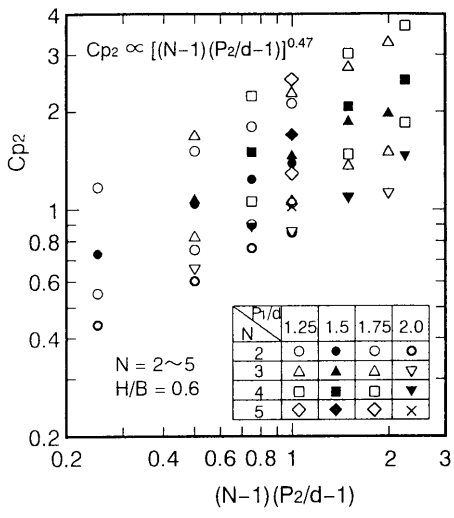


(a) Correlation of Cp_3 vs N

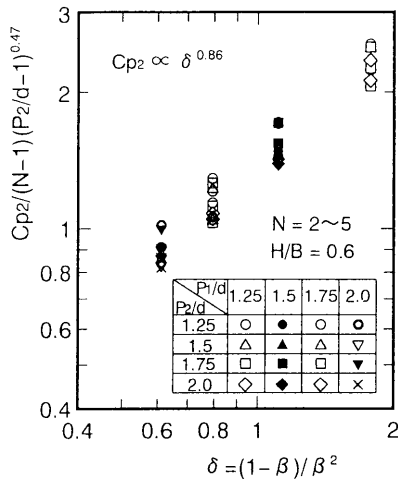


(b) Correlation of Cp_3 vs δ

Fig. 6 Pressure raise at outlet



(a) Correlation of C_{p2} vs $(N - 1)(P_2/d - 1)$



(b) Correlation of $C_{p2}/(N - 1)(P_2/d - 1)$ vs δ

Fig. 7 Pressure drop between inlet and outlet

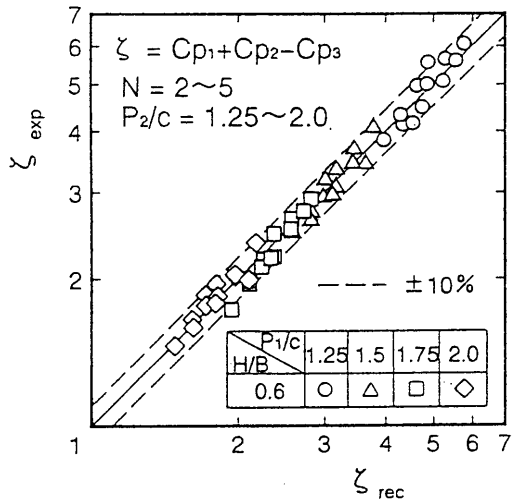
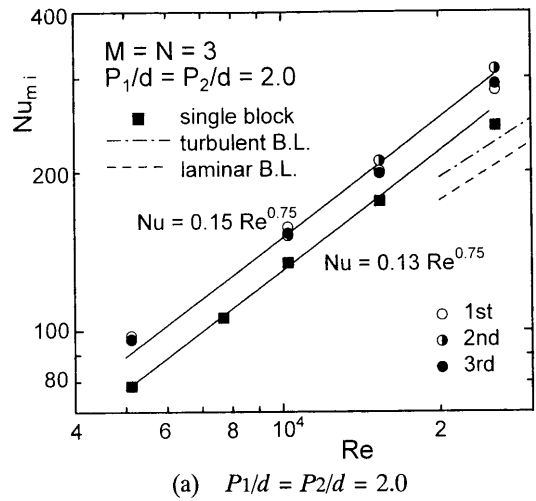


Fig. 8 Pressure loss coefficient ζ

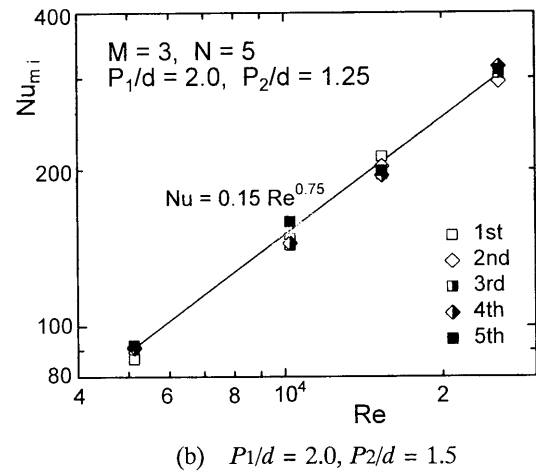
$$Num_L = 0.38 Re^{0.62} \quad (\delta L/H = 0.06 \sim 0.13) \quad (8-1)$$

$$Num_T = 0.42 Re^{0.62} \quad (\delta T/H = 0.52 \sim 1.52) \quad (8-2)$$

where, δL and δT are laminar and turbulent boundary layers



(a) $P_1/d = P_2/d = 2.0$



(b) $P_1/d = 2.0, P_2/d = 1.5$

Fig. 9 Mean Nusselt number ($M = 3$)

thickness. The Nusselt number of the present experiment is slightly higher than that in a turbulent boundary layer. For the case of $M = 3, N = 3 \sim 5$, the Nusselt number of i -th row block, Num_i , can be approximately expressed by

$$Num_i = 0.15 Re^{0.75} \quad (P_1/d = P_2/d = 1.25, i = 1 \sim 5) \quad (9)$$

Figures 10 (a) and (b) show examples of the cases of $M = 4$ and 5, respectively. For the case of $M = 4$, the Nusselt number of 1st row block is lower 15 % than those of downstream blocks. On the downstream blocks, there is no significant difference in N and i . The Nusselt number of the i -th row block can be approximately given by

$$Num_1 = 0.16 Re^{0.75} \quad (P_1/d = P_2/d = 1.25, i = 1) \quad (10-1)$$

$$Num_i = 0.18 Re^{0.75} \quad (P_1/d = P_2/d = 1.25, i = 2 \sim 5) \quad (10-2)$$

$$Num_i = 0.19 Re^{0.75} \quad (P_1/d = P_2/d = 1.25, i = 1 \sim 5) \quad (11)$$

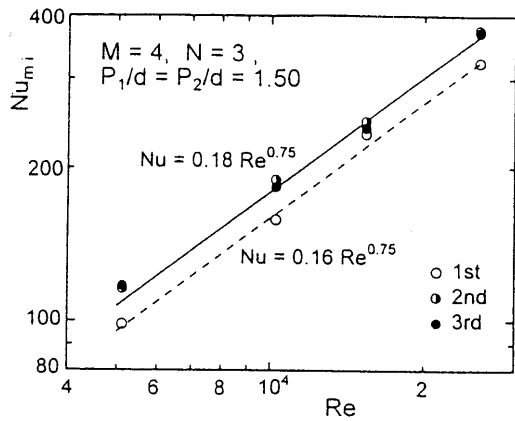
For all arrangement, the Nusselt number of individual block is proportional to $Re^{0.75}$. And the Nusselt number increases with an increase in M . This fact is caused by an increase in flow velocity around blocks due to the high blockage effect in the flow path. We try the formulation of the Nusselt number considering the blockage effect.

Introducing the opening ratio β , the modified Reynolds number is defined by $Re^* = Re/\beta$. For the cases of $M = N = 3, 4$ and 5 , the Nusselt numbers are rearranged by Re^* , and are shown in Fig. 11. For single block and i -th row block in array, all experimental data is approximately expressed within 10 % as follows:

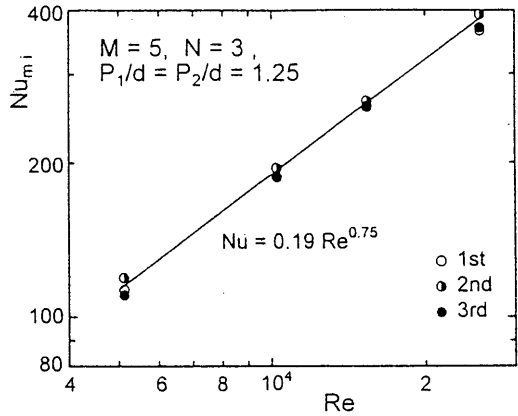
$$Nu_{mi} = 0.118 (Re/\beta)^{0.75} \quad (\beta = 0.52 \sim 0.72) \quad (12)$$

4.2 Correlation between heat transfer and pressure loss

Next, we discuss the correlation between the heat



(a) $M = 4, P_1/d = P_2/d = 1.5$



(b) $M = 5, P_1/d = P_2/d = 1.25$

Fig. 10 Mean Nusselt number ($M = 4, 5$)

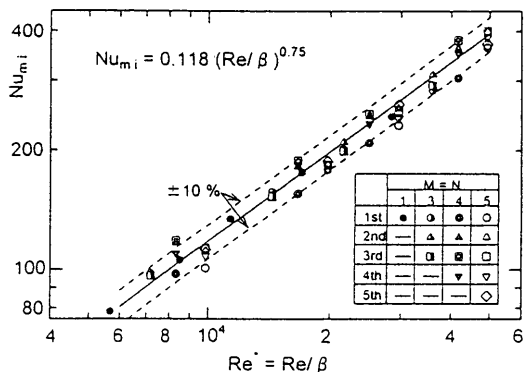


Fig. 11 Mean Nusselt number arranged by modified Reynolds number

transfer and pressure loss. The pumping power, P_w , is one of the performance assessment and which is defined by

$$P_w = \Delta p \cdot BW \cdot U_m \quad [\text{Watt}] \quad (13)$$

where, $BW \cdot U_m$ is the flow rate and Δp is the pressure drop between inlet and outlet of the array of blocks. The Δp is a measured value or a calculated value by $\zeta \cdot 0.5\rho U_m^2$. The sum of Nu_{mi} is the total heat flow rate Nu_{total} and the average Nusselt number per block, Nu_{ave} , is given by

$$Nu_{ave} = \frac{\sum_{i=1}^N Nu_{mi}}{N} \quad (14)$$

The correlations P_w vs Nu_{total} is shown in Fig. 12. The pumping power is proportional to the number of blocks and the total Nusselt number is also proportional to $[P_w]^{1/4}$. From Eqs. (13), the pumping power P_w is proportional to U_m^3 , so the dependency of Reynolds number is coincide with those of Eqs. (9) ~ (11). In the range of $\beta = 0.52 \sim 0.72$, a high density array is successful for the heat transfer performance. The correlation between the average Nusselt number of i -th row blocks in an array and the pumping power of the array is shown in Fig. 13. The following correlation equation is obtained:

$$Nu_{ave} = 190 [P_w]^{0.25} \quad (i = 2 \sim N) \quad (15)$$

4.3 Dimensionless correlation equation

The dimensions of both sides of Eq. (15) are not equal. Then, we try to obtain the dimensionless correlation equation from dimensional analysis. The physical quantities concerning this heat transfer phenomena are as follows:

$$hm = f(U_m, d, H, P_1, P_2, B, W, \mu, \rho, C_p, \lambda) \quad (16)$$

where, μ, ρ, C_p and λ are physical properties. And the parameters H, P_1, P_2, B and W are included in the pressure difference Δp , then these terms are replaced by Δp .

$$hm = f(U_m, d, \Delta p, \mu, \rho, C_p, \lambda) \quad (17)$$

The dimensional analysis leads us to the next correlation.

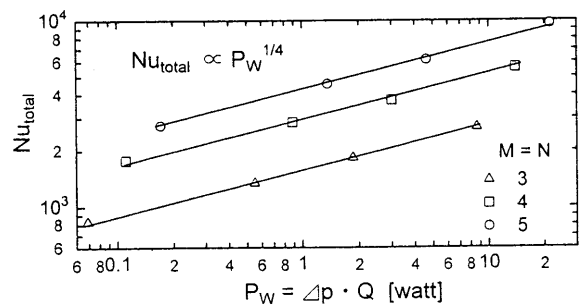


Fig. 12 Correlations total Nusselt number vs pumping power

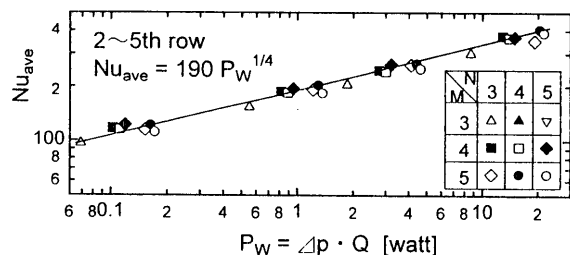


Fig. 13 Correlations average Nusselt number vs pumping power

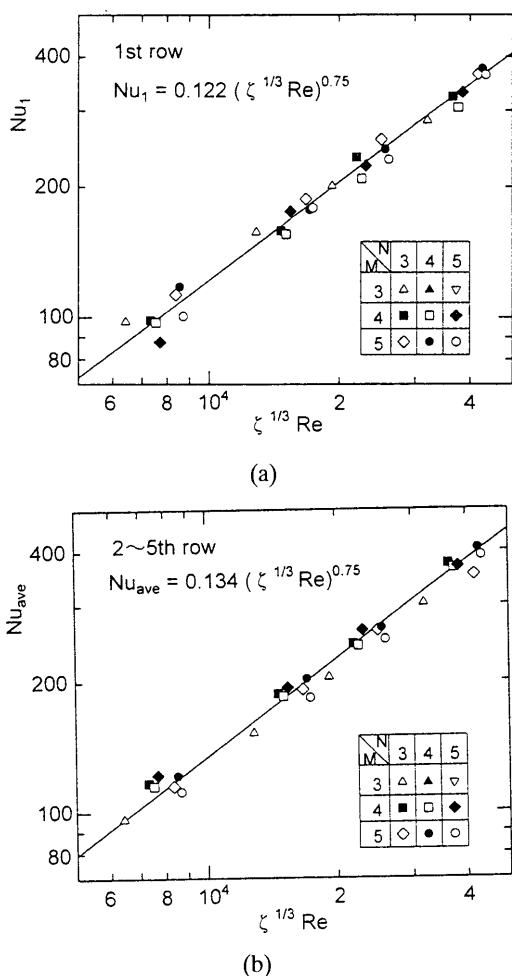


Fig. 14 Dimensionless expression

$$hmd/\lambda = f(\Delta p/\rho Um^2, Umd/(\mu/\rho), \mu Cp/\lambda) \quad (18)$$

The above four dimensionless groups are Num , ζ , Re and Prandtl number Pr , respectively. Prandtl number of air is nearly constant. Then, the following equation is obtained.

$$Num = f(\zeta, Re) = C \zeta^m Re^n \quad (19)$$

Equations (15) lead to the exponents, $m = 0.25$, $n = 0.75$. Therefore, Eq. (19) is rearranged by

$$Num = C (\zeta^{1/3} Re)^{0.75} \quad (20)$$

The above correlations for all experimental data are shown in Fig. 14. The average Nusselt numbers of 1st row and 2nd to 5th rows blocks are represented by the following dimensionless expressions, respectively.

$$Nu_{ave} = 0.122 (\zeta^{1/3} Re)^{0.75} \quad (i = 1) \quad (21)$$

$$Nu_{ave} = 0.134 (\zeta^{1/3} Re)^{0.75} \quad (i = 2 \sim N) \quad (22)$$

The above equations agree well with the experimental data within $\pm 5\%$.

5. CONCLUSIONS

The results led to the following conclusions:

- (1) The pressure loss coefficient ζ , can be expressed as the summation of the coefficients of pressure drop at the inlet part and intermediate part of the array, $Cp1$, $Cp2$ and pressure raise at the outlet part of the array $Cp3$:

$$\zeta = Cp1 + Cp2 - Cp3$$

The individual coefficients are formulated as follows:

$$Cp1 = 2.86 \delta^{0.76} (P2/d)^{-0.23},$$

$$Cp2 = 1.40 \delta^{0.86} [(N-1)(P2/d-1)]^{0.47},$$

$$Cp3 = 1.13 \delta^{0.47} [(N-1)/(P2/d)^2]^{0.09}.$$

- (2) The average heat transfer of single block is slightly higher than that of block in a turbulent boundary layers.
- (3) The average heat transfer of the 1st row is lower about 10% than those of 2nd to 5th rows. As an increase in M and N , the heat transfer increases due to the blockage effect.
- (4) The average heat transfer of i -th row block expressed by the following equation using the opening ratio β .

$$Num_i = 0.118 (Re/\beta)^{0.75} \quad (\beta = 0.52 \sim 0.72)$$
- (5) The correlation between the average Nusselt number and the pumping power is given by

$$Nu_{ave} = 190 (Pw)^{0.25} \quad [Pw: \text{Watt}]$$
- (6) Introducing the pressure loss coefficient, ζ , the above equation is rewritten to dimensionless expression:

$$Nu_1 = 0.122 (\zeta^{1/3} Re)^{0.75},$$

$$Nu_{ave} = 0.134 (\zeta^{1/3} Re)^{0.75}.$$
- (7) In the range of present blockage ratio, a high density array is successful for the heat transfer performance.

ACKNOWLEDGEMENTS

The authors wish to thank Mr. T. Hiraoka of the former student of the National Defense Academy for his assistance in the heat transfer experiments.

REFERENCES

1. JSME Handbook on Cooling Design of Electronic Equipment (in Japanese), (1995).
2. Mohat R. T., Arvizu D. E. and Ortega A., Cooling electronic components: forced convection experiments with an air-cooled array, Heat Transfer Equipment, HTD, Vol. 48, ASME/AIChE Annual Heat Transfer Conference (1985), pp. 17-27.
3. Matsushima, H., Yanagida, T. and Nakayama, W., Pressure Drop Characteristics of Circuit Board with Arrays of LSI Package, Trans. Jap. Soc. Mech. Engr., Vol. 59, No. 560, B (1993), pp.1244-1251.
4. Igarashi, T. and Fukuoka, T., Pressure Drop of Arrays of In-line Blocks on the Wall of Parallel Channel, Trans. Jap. Soc. Mech. Engr., Vol. 66, B (2000), to be published.
5. Tsutsui, T., Igarashi, T. and Nakamura, H., Fluid Flow and Heat Transfer around a Cylindrical Protuberance Mounted in a Flat Plate Boundary Layer, Trans. Jap. Soc. Mech. Engr., Vol. 65, No. 633, Ser. B (1999), pp. 1716-1723. or JSME International J., Vol. 43, No. 2, Ser. B (2000), to be published.
6. Igarashi, T., Flow Resistance of a Vortex Shedder in a Circular Pipe, Proc. of Fifth Triennial Int. Symp. on Fluid Control, Measurement and Visualization, Hayama (1997), pp. 743-748.
7. Igarashi, T., Hydraulic Losses of Flow Control Devices in Pipes, JSME International J., Vol. 38, No. 3, Ser. B (1995), pp. 398-403.